Progress Report - 31 July 2023

Arba Shkreli

July 2023

1 Introduction

At this stage, now that I have a fully initiated means for running experiments, I can dedicate more time towards coming up with approaches to address the problem of acquiring sharper and user-friendly images of objects underground, which I will introduce shortly.

As noted previously, A and B-scans plot the intensity of incoming waves versus the time after the initial pulse was thrown by the GPR. Without knowing the exact characteristics of the materials the waves encountered, determining the depth from which the reflections come becomes a matter of trying to estimate the material characteristics in real-time, which is challenging due to the soil's heterogeneity and not within the scope of this project.

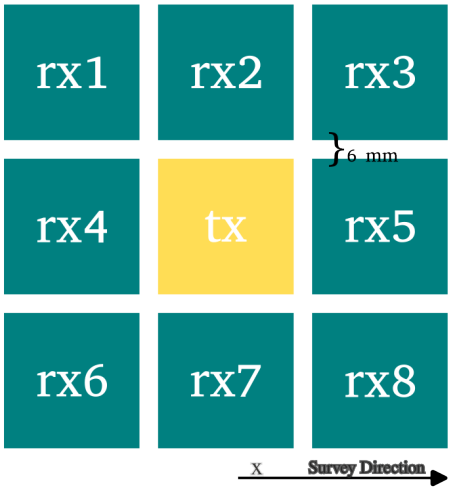

Figure 1: Antenna configuration used

We will effectively increase aperture size by attributing many receivers to one transmitter. In this single-transmitter, multi-receiver layout, we will perform what is called a common offset survey, meaning that the relative distance between each receiver and the transmitter remains the same as the whole array moves across the ground. Each receiver will generate its own B-scan. The goal is to merge all of the B-scans first to obtain one very detailed B-scan.

What is the reasoning for this antenna setup? The heterogeneity and mixed nature of the medium we are radiating means that significant scattering in 3D will take place. That is, even though the original pulse we transmitted is perpendicular to the ground, the reflections will propagate in various directions.

This week we placed a PMA landmine model 15 cm in the ground, and took a B-scan over it with an array of 8 receivers and 1 transmitter 5 cm above the ground. Obtaining 8 B-scans, I wanted to figure out how to best merge the B-scans into one "good" B-scan, the idea being that what one receiver got another did not. The receivers captured the z component of the E field, or the one parallel to the pulse's polarization, as that is the most significant component that they would capture anyway.

The raw results are displayed on the next page. At least visually, it looks like the notion of adding the components of each B-scan could generate a complete picture. What we will do first is naively add the components with equal weight. It remains to see if this is a reasonable approach, as I try to consult literature and experts on the topic.

One question that remains is why Receivers 4 and 5 had such as scattered mosaic pattern compared to the others. They are the receivers that lie along the direction of the motion of the antenna array. However, I do not see why such a noisy picture would be generated by either, because over the course of each A-scan taken, the antenna array does not move, so they should not be that different from the others. I will investigate to see if maybe something in the setup was described incorrectly, or if there is a theoretical misunderstanding/misconception I am having. The relative position of the receivers is also described by Figure 1.

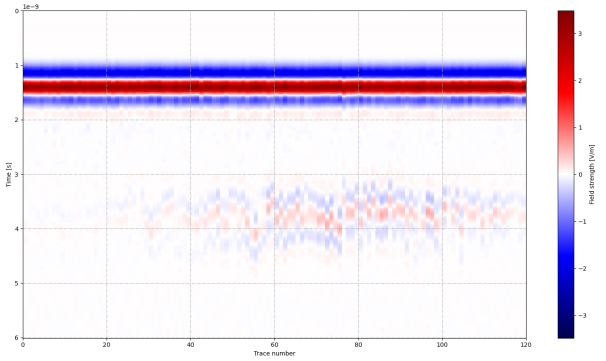

(a) Receiver 1

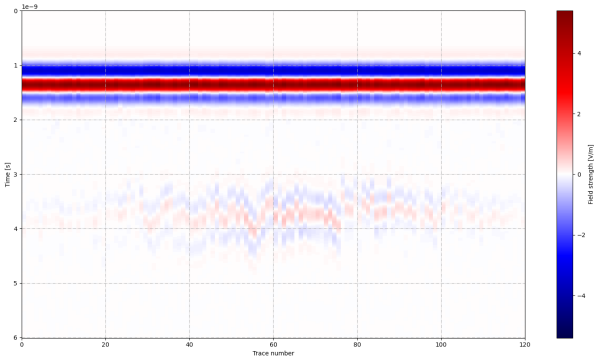

(b) Receiver 2

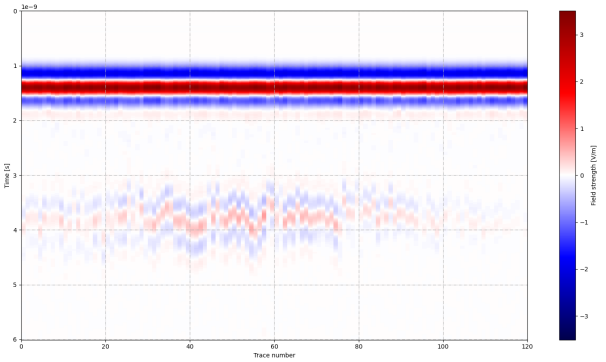

(a) Receiver 3

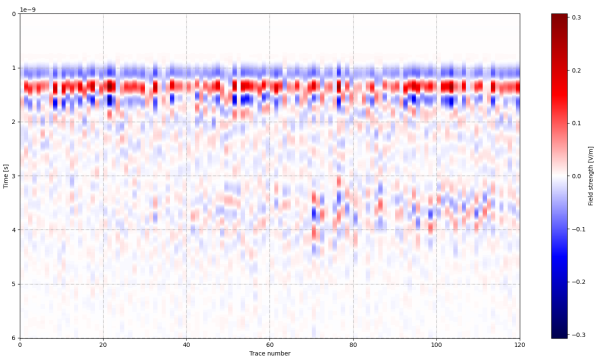

(b) Receiver 4

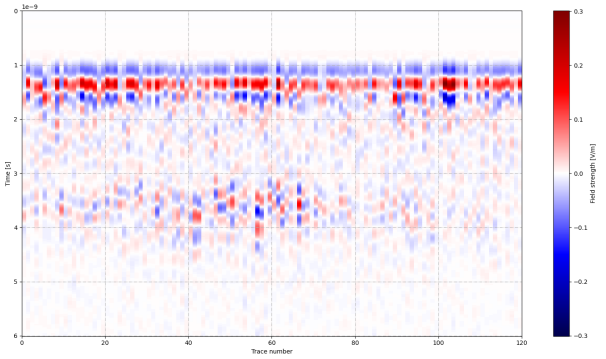

(a) Receiver 5

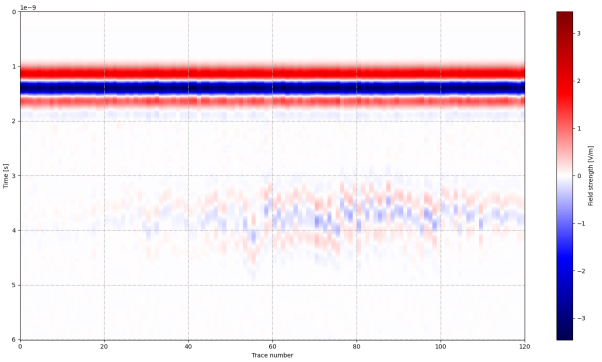

(b) Receiver 6

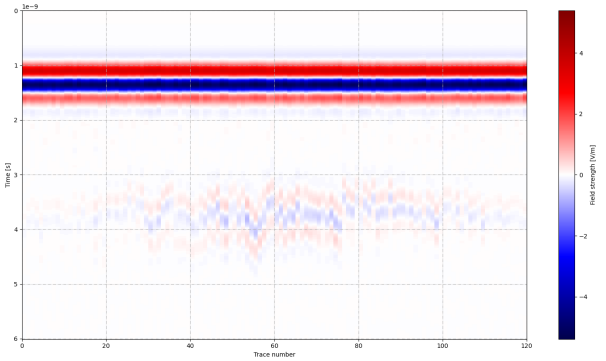

(a) Receiver 7

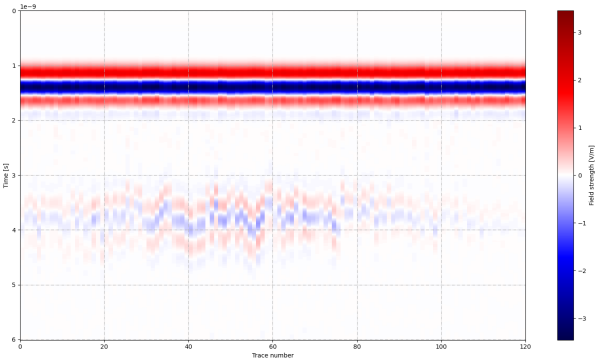

(b) Receiver 8

2 Processing Raw Data

gprMax generates HDF5 files (a format used for large datasets in some contexts) as outputs for each simulation, which I settled to use the 'h5py' Python package to work with, as that had also been the choice of the gprMax developers. What I tried first was going for the perhaps naive approach to combine the data seen in the figures: simply adding the corresponding values in the B-scans. I merged them both as raw values to generate one merged scan (Figure 7), and also absolute values (Figure 9) to see if perhaps there is difference in how we could infer features one way or the other. Another transformation that was performed was taking the average of one A-scan at a time and subtracting that from each point in the A-scan (known as a "zero-offset" removal, see [BTBD17]). This aids in the removal of some background "DC" noise, but another method I would like to explore uses SVD ([LSL17]).

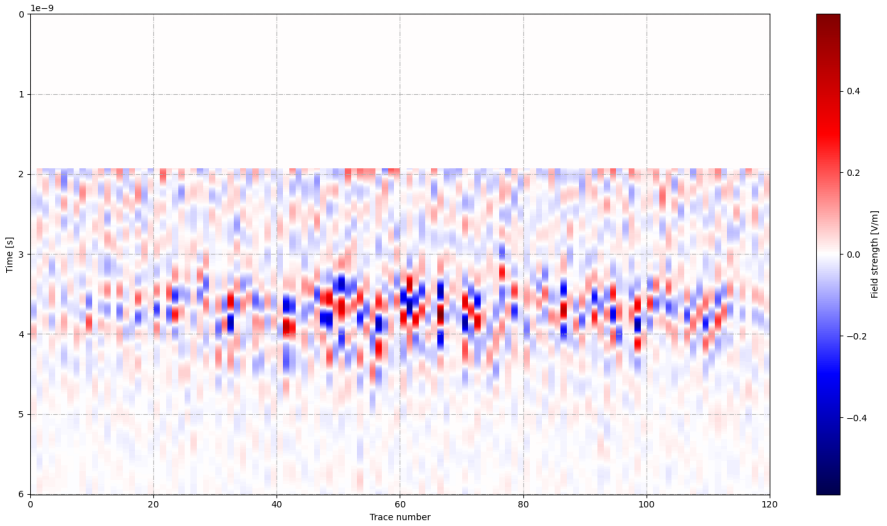

Figure 6: Merged raw value B-scans, top bands removed, no zero-offset removal

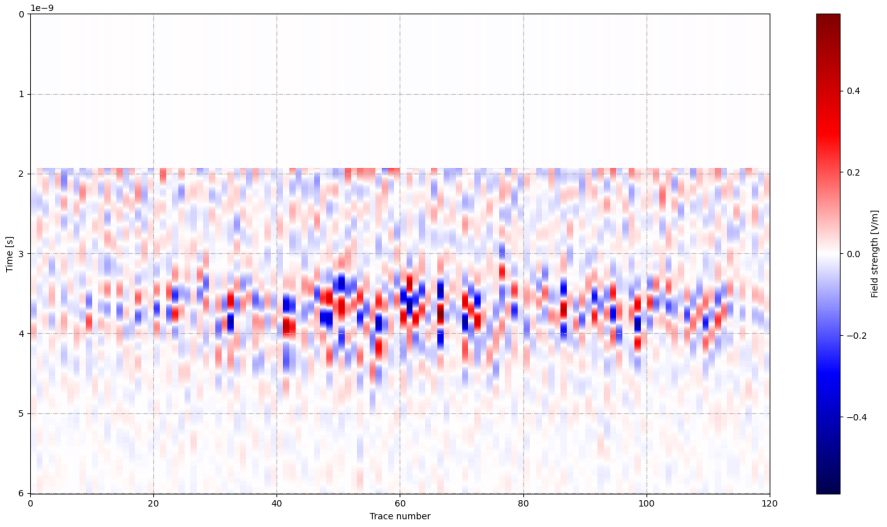

Figure 7: Merged raw value B-scans, top bands removed, zero-offset removal

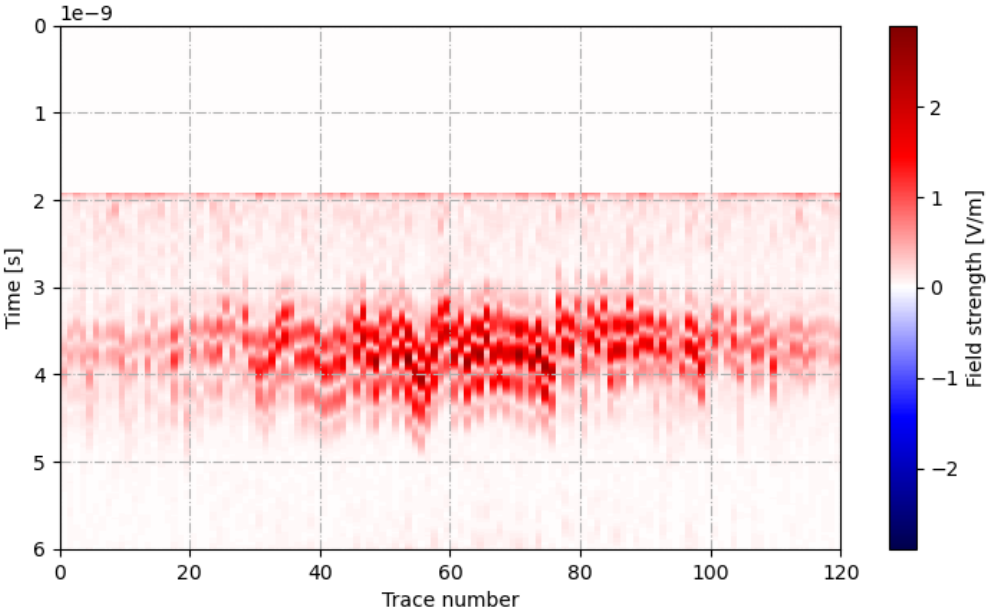

Figure 8: Merged absolute value B-scans, top bands removed, no zero-offset removal

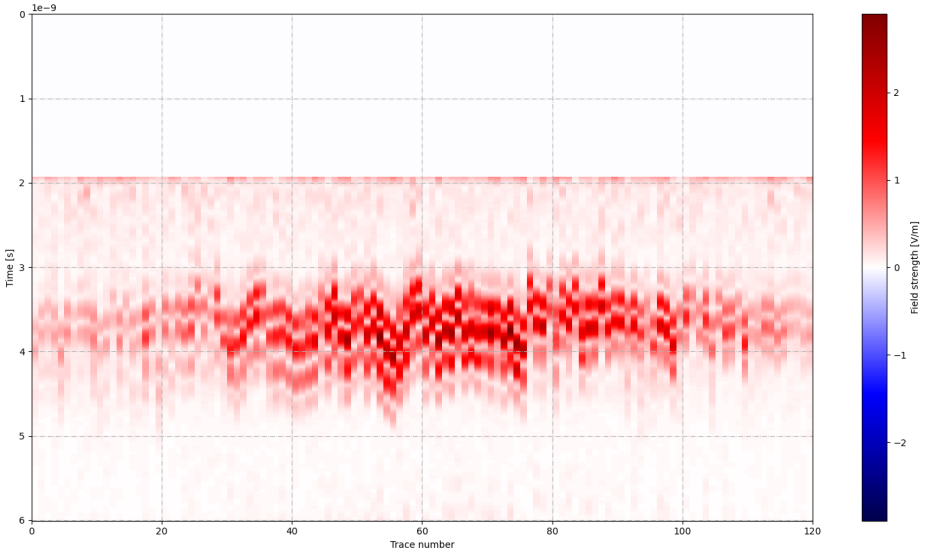

Figure 9: Merged absolute value B-scans, top bands removed, zero-offset removal

Zero-offset removal does not offer substantial improvement in the images, so SVD denoising and other methods must be explored. The next steps will also be to see if there are better ways to combine the data besides equal-weight adding, and then use the combined B-scans to infer more about what lies underneath. Promising literature regarding the determination of tree root shapes underground using GPR is from where I will take inspiration next ([ASL21]).

References

[ASL21] Abderrahmane Aboudourib, Mohammed Serhir, and Dominique Lesselier. A processing framework for tree-root reconstruction using ground-penetrating radar under heterogeneous soil conditions. *IEEE Transactions on Geoscience and Remote Sensing*, 59(1):208–219, 2021.

[BTBD17] Andrea Benedetto, Fabio Tosti, Luca Bianchini Ciampoli, and Fabrizio D'Amico. An overview of ground-penetrating radar signal processing techniques for road inspections. *Signal Processing*, 132:201–209, 2017.

[LSL17] Cai Liu, Chao Song, and Qi Lu. Random noise de-noising and direct wave eliminating based on svd method for ground penetrating radar signals. *Journal of Applied Geophysics*, 144:125–133, 2017.